Direct-Inverse Transonic Wing Analysis-Design Method with Viscous Interaction

Leland A. Carlson*
Texas A&M University, College Station, Texas
and
Richard A. Weed†
Lockheed-Georgia Company, Marietta, Georgia

A direct-inverse transonic wing analysis-design method which includes the effects of viscous interaction due to a turbulent boundary layer is presented. The method, based upon the fully conservative ZEBRA II transonic potential flow algorithm, uses a Cartesian-like grid system, and includes automatic relofting to control the amount of trailing-edge thickness at each design station. Viscous interaction is included by a two-dimensional boundary layer scheme modified to account for the first-order effects of three-dimensionality. Comparisons with experimental data are presented which verify that this method improves transonic aerodynamic studies associated with preliminary design and analysis.

Introduction

In recent years, the increasing importance of transonic flight by both military and commercial aircraft has prompted significant efforts to develop more accurate and reliable computational methods for the design and analysis of aircraft components, particularly wings, in transonic flow. A strong motivation for this research has been the increasing cost of wind tunnel tests and the interference and scale problems associated with tests conducted at transonic conditions. As a result, several computer codes have been developed to design transonic wings which satisfy certain specified flow conditions.[1-4]

One design technique which has been successfully used is the inverse approach. In this method, the wing geometry is computed by specifying a desired pressure distribution over part of the wing and then solving the mixed Neumann and Dirchlet boundary value problem by finite difference techniques. Since the inverse technique utilizes pressure distributions, which can easily be tailored to satisfy desired flight conditions, as input and since it can be applied to either the entire wing or a portion of the wing, this method may be simpler to use and more cost effective than other numerical procedures. However, the speed of the inverse method depends upon the efficiency of the solution scheme. Recently, a combined direct-inverse three-dimensional transonic wing design method,[4] suitable for use on either vector of sequential computers, was developed. This method uses the direct-inverse approach in a Cartesian-like grid system, solves the inviscid full-potential equation in conservative form, and has proven to be fast, reliable, and accurate. In addition, it includes an automatic relofting technique that permits the user to control the amount of trailing-edge thickness at each span station being designed.

Unfortunately, at transonic speeds, experimental evidence[5,6] indicates that viscous interaction effects can significantly affect both the pressure distribution on a wing and the resultant aerodynamic force coefficients. For example, a wing using aft-cambered airfoil sections, which were designed inviscidly for transonic conditions, might actually develop in practice 25–50% less lift than predicted by an inviscid design procedure. This loss in lift would primarily be due to the existence of the boundary layer on the wing which "displaces" the inviscid flow and changes the effective shape of the wing. In addition, other viscous phenomena, such as wake curvature and vertical pressure gradients in the trailing-edge wake region, also affect the wing aerodynamic coefficients. To prevent serious discrepancies, the effects of at least weak viscous interaction should be included in both the analysis and design portions of any transonic analysis-design numerical method. It should be noted that the term "weak viscous interaction" implies that there is no massive boundary layer separation anywhere on the wing. Nevertheless, for many wings at transonic conditions, the effects of weak viscous interaction on wing performance can still be large.

Consequently, an effort was initiated to modify the direct-inverse three-dimensional transonic wing design code and method of Ref. 4 to include the effects of weak viscous interaction. Specifically, the objectives of this effort were as follows:

1) Select and, where appropriate, modify a turbulent boundary layer calculation suitable for the transonic analysis-design problem.

2) Incorporate the selected method into the analysis-design computer code.

3) Determine the operational and convergence characteristics of the resultant viscous analysis-design transonic method.

4) Verify the overall validity of the method.

Finally, it should be noted that the overall goal of this project was to develop a method and computer code suitable for applied engineering usage in the area of preliminary transonic wing design.

Problem Formulation

In the present effort, the basic approach was to assume that the three-dimensional inviscid flowfield follows a viscous displacement surface having ordinates and slopes different from those of the actual wing. It is true that an inviscid flowfield does not exactly follow the displacement surface in the vicinity of the trailing edge of a wing and is also influenced by the effects of wake curvature; such effects were, however, assumed in the present approach to be either secondary or capable of being handled empirically.

Presented as Paper 85-4075 at the AIAA 3rd Applied Aerodynamics Conference, Colorado Springs, CO, Oct. 14-16, 1985; received Nov. 11, 1985; revision received May 29, 1986.

*Professor, Aerospace Engineering Department. Associate Fellow AIAA.

†Associate Scientist, Advanced Flight Sciences. Member AIAA.

At those wing stations where the wing was designed using the inverse procedure, the approach was to treat the airfoil sections determined by the inverse technique as the displacement surfaces for those sections, and to subtract from them the displacement thicknesses determined by a boundary layer computation. Normally, this subtraction was performed after the inverse design procedure had converged, and the resultant ordinates were considered to be the actual wing ordinates at the designer stations.

For those parts of the wing which were not being designed and for which the actual wing ordinates were known, viscous interaction was included as if those portions were being analyzed (i.e., wing ordinates given and flowfield and pressure distribution to be determined). At these analysis stations, the approach was to calculate a boundary layer displacement surface (i.e., wing ordinate plus displacement thickness) and then to compute the inviscid flowfield using the resultant displacement surface. Since viscous interaction can significantly affect the pressure distribution and flowfield, the computation of the boundary layer and the displacement surface at the analysis stations was performed at regular intervals throughout the iterative computation of the inviscid flowfield. In this manner, the convergence rate was enhanced, and the final solution reflected the effects of viscous interaction in a coupled manner.

For the inviscid portion of the flowfield, the full-potential, fully conservative direct-inverse transonic wing design code developed previously[4] was utilized. In this scheme, the computational grid was a stretched Cartesian grid system which had been sheared to align it with the leading and trailing edges of the wing. One advantage of this sheared grid system was that each spanwise plane of the grid contained an equal number of points on or adjacent to the wing surface. In addition, the wing surface was covered with an evenly spaced grid system. Off the wing, the regions in front of the leading edge, behind the trailing edge, and outboard of the wing tip were stretched exponentially, while geometric stretching was used above and below the wing mean plane.

In a typical analysis or design solution, a sequence of three X, Y, Z grids was used, starting with a $25 \times 30 \times 8$ grid and finishing on a $90 \times 30 \times 30$ grid. In all cases, 20 stations were placed on the half span of the wing; for the fine grid, 50 chordwise points were located between the local leading and trailing edges at each span station for both the upper and lower surfaces.

For the inviscid portion of the flowfield, the full potential equation in fully conservative form was solved using the retarded density approximation and the ZEBRA II algorithm developed by Keller, South, and Hafez.[7] Whenever possible, the scheme was coded in a manner which would permit efficient vectorization. In addition, the full wing surface boundary conditions in either the analysis or design case were applied on the wing mean plane, since previous investigations[8,9] had shown that excellent accuracy could be obtained with this approach. Further, by using the Cartesian grid system with mean-plane boundary conditions, the computational grid did not have to be recomputed each time the wing shape or its displacement surface was recomputed.

For complete details and examples concerning the inviscid direct-inverse transonic wing design and analysis method, see Refs. 4 and 10.

Viscous Interaction

The primary task of the effort was to include viscous interaction in the inviscid analysis-design method, and the key to properly including viscous effects was to select and incorporate a boundary layer computational method which accurately yielded displacement thicknesses and the resultant displacement surfaces. Such a boundary layer scheme had to be reliable, reasonably accurate, and computationally very efficient. The latter requirement was considered to be very important since, in the analysis regions, the boundary layer had to be updated many times throughout a complete calculation in order to properly couple the viscous and inviscid portions of the flowfield. In addition, the viscous method had to be computationally robust in the sense that it could not fail or cause the program to terminate computations when phenomena such as premature separation occurred near the trailing edge of the wing or in the vicinity of shock waves. Frequently, such effects do occur during the initial stages of computation, particularly near shock waves and in the cove region on aft-cambered airfoils, although they do not exist in the final converged solution.

Many possibilities existed during the selection of an appropriate boundary layer method. Obviously, the most complicated and perhaps most accurate choice would have been a fully three-dimensional turbulent compressible technique. However, such methods were found to be computationally intensive, expensive, and time consuming; in most cases they had not been extensively validated against transonic experimental data. Also, it would have been difficult to couple such methods to the existing inviscid transonic computational scheme. Consequently, three-dimensional methods were considered unsuitable for inclusion in the present analysis-design technique, which was intended primarily for use in preliminary design.

At the other extreme, the simplest approach would have been to use a simple, proven, two-dimensional compressible turbulent boundary layer method and to apply it using straightforward two-dimensional strip theory at the various wing stations. While this approach had been used by previous investigators,[11] and certainly would have given an indication of viscous interaction trends, evidence[12] indicated that it would underpredict the magnitude of the displacement thickness. Nevertheless, the idea of using a two-dimensional technique was attractive from the standpoint of computational efficiency.

Approximately a decade ago, Nash and Tseng[12] investigated the possibility of using two-dimensional techniques to compute the turbulent boundary layer on an infinite yawed wing. By comparing two-dimensional results with three-dimensional calculations, they determined that a two-dimensional calculation performed normal to the wing leading edge yielded good results for the variation and magnitude of the displacement thickness. On the other hand, their results showed that a calculation carried out in the streamwise direction seriously underpredicted the magnitude of the displacement thicknesses, primarily because such an approach sensed pressure gradients considerably less than those effectively influencing the actual boundary layer growth. Based on these conclusions, Nash and Tseng modified the governing boundary layer equations and devised a technique which used a two-dimensional calculation normal to the wing leading edge and which yielded results in excellent agreement with three-dimensional computations on a yawed infinite span wing. They referred to this method as a "modified chord technique."

Based on the results of Nash and Tseng, it was decided to use in the viscous portion of the present analysis-design wing program a two-dimensional boundary layer scheme suitably modified to account for at least the first-order effects of three dimensionality on viscous interaction. Thus, in the present method, it was inherently assumed that at least locally the boundary layer growth and behavior on the wing was like that on an infinite swept wing. This approach had the advantage of being able to utilize a verified and robust two-dimensional turbulent boundary layer scheme that was computationally efficient, and it was believed that it would be adequate for wings of moderate and medium sweep.

Unfortunately, the modified chord technique was not directly suitable for incorporation into the existing analysis-design program in that it solved a system of partial differential equations and was time consuming. Also, it was only strictly applicable to incompressible flow, and its usage would have required extensive interpolation and extrapolation to deter-

mine the pressure and coordinates along lines normal to the leading edge (or the average sweep line) since the computational grid was aligned with the freestream. Such extrapolations could introduce inaccuracies which might obliterate any attempt at improvement. On the other hand, Nash and Tseng showed that a streamwise computation predicted incorrect displacement thicknesses simply due to the usage of inaccurate pressure gradients.

Consequently, it was decided to use a streamwise direction two-dimensional turbulent boundary layer calculation method that was modified to utilize effective pressure gradients at the various wing stations. Based upon wing sweep theory and the results of Nash and Tseng, such a correction involved increasing the streamwise pressure gradients by a factor of one over the cosine squared of an appropriate average sweep angle. While this approach was an approximation, it was felt that it would yield good values for the displacement thicknesses and would be a significant improvement over results obtained using simple strip theory. In addition, this technique should be adequate for preliminary analysis and design, and its accuracy should be compatible with that associated with assuming point transition to turbulent flow.

After extensive investigation of various two-dimensional turbulent boundary layer methods, the Nash-Macdonald method,[13] together with the modified pressure gradient approximation and certain smoothing operations, was selected for incorporation into the analysis-design program. This method was selected because it yielded excellent predictions of displacement thicknesses in two-dimensional transonic flows and because of its computational robustness and efficiency. In this method, the displacement thickness at the trailing edge of a spanwise station was always determined by linear extrapolation from the previous two upstream grid point values. As a result, the basic approach was similar to that used in the two-dimensional transonic inverse analysis-design program TRANDES[14] as well as the low-speed high-lift program TRANSEP.[15]

To update the displacement surface, the momentum integral equation was solved for the momentum thickness using the formulas of Nash and Macdonald for the skin friction and the shape factor. However, the pressure used as input into the momentum integral equation was obtained from the current inviscid solution and modified as previously discussed so as to yield the effective pressure gradients influencing the boundary layer growth. This computation was performed on the same grid spacing as the corresponding inviscid solution. The resultant displacement thicknesses were smoothed and then extrapolated to obtain the thicknesses at the trailing edge. Normally, this smoothing was performed twice on the medium grid and four times on the fine grid each time the boundary layer was computed.

The smoothing and extrapolation process had two advantages. First, it reduced the rapid variations in the solution which sometimes occured in regions with high pressure gradients. Second, based on comparisons with two-dimensional experiments, this approach yielded a behavior that was correct with respect to the growth of the boundary layer in the trailing-edge region and the subsequent effect on the pressure distribution and lift. Consequently, it was believed that this method would be a reasonable engineering model in a preliminary design code.

As a result of numerical experiments, it was determined that it was inefficient and inappropriate to include viscous interaction on coarse grids due to the inherent pressure and flowfield inaccuracies associated with such grids. Consequently, the viscous interaction procedure was not normally initiated until the 50th cycle of the medium grid. At that point, the displacement thicknesses were computed at each appropriate wing station (i.e., analysis stations) at the same chordwise coordinates as the inviscid grid, and the displacement surface ordinates were updated using under-relaxation.

For the cases where relofting was also included, it was found best not to start the relofting procedure until about the 100th cycle of the medium grid. At that point, the solution was normally sufficiently converged to permit reasonably accurate calculation of the airfoil sections at the design stations. Based upon these airfoil shapes, the ordinates in the direct region (i.e., leading edge) of each design station were recomputed using the procedure developed in Ref. 4. This approach opened or closed the leading edge of each design section; and, in conjunction with the prescribed pressure distribution at the design stations and the inverse procedure, it effectively controlled the amount of trailing-edge closure.

Subsequently, the chordwise and spanwise slopes were determined from cubic splines through the new displacement surface and relofted ordinates, and the wing surface boundary conditions for the airfoil sections at the analysis stations and the direct portion of the design stations of the wing were recalculated. Of course, at the design stations and design pressure coefficients determined the appropriate boundary conditions. Normally, boundary layer calculations, relofting, and ordinate updates were performed every 10 iteration cycles thereafter. The actual start of the boundary layer and relofting calculations and the frequency of updating were, however, controllable by the user via input parameters.

It should be noted that while this approach did properly account for the effects of weak viscous interaction at both analysis and design wing stations, no attempt was made to account for massive separation at the wing trailing edge or at the shock wave. Since the present method was primarily intended as a design tool, it was considered unlikely that an aerodynamicist would deliberately attempt to design transonic wing with extensive trailing edge or shock-induced separation. Additionally, it should be noted that this method cannot always be used to design a physically reasonable wing for a completely arbitrary wing pressure distribution. Like almost all direct-inverse techniques, the utility of the present method is in the modification of initial designs, using reasonable pressure distributions that are based upon experience.

Convergence Characteristics

An ONERA M-6 wing at a Mach number of 0.84 and an angle of attack of 3.06 deg was the primary test case used to develop the viscous analysis and design options in the present method and to determine the convergence characteristics of the program. The ONERA wing, which has an aspect ratio of 3.8, a taper ratio of 0.56 and is composed of symmetrical airfoil sections, was selected because it was typical of low-aspect ratio-type wings. In addition, quality experimental data were available for the wing and it had been used by other investigators as a standard test case for new computer programs.

In order to establish the existence of convergent behavior, the maximum residual, average residual, and maximum potential change were monitored; and, in addition, tests were performed on a variety of machines. In all cases the maximum residual was reduced by several orders of magnitude on each

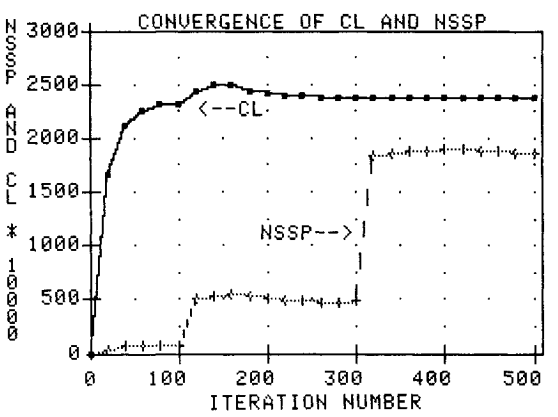

Fig. 1 Variation of lift coefficient and the number of supersonic points iteration number.

grid, and it was established that converged engineering results could be obtained by the usage of 100 coarse grid, 200 medium grid, and 200 fine grid iterations.

In addition to residual variation, the number of supersonic points and the value of the lift coefficient were monitored as an additional indication of convergence. Figure 1 shows the variation of these properties with iteration number for a typical analysis-design case. The increase in the number of supersonic points at iterations 100 and 300 was due to grid halving and, as can be seen, both the lift coefficient and the number of supersonic points stabilized prior to the end of the computations on each grid. These results further verified that the present method and procedure did converge adequately for engineering usage.

Since the present method incorporated the effects of weak viscous interaction, it was essential to establish that the viscous portions of the calculations converged as well. Figure 2 portrays the variation in the upper surface trailing-edge ordinates of the fluid airfoil (i.e., actual airfoil plus displacement thickness) at two analysis span stations for a typical analysis-design case. Since the viscous calculations were not started until the 50th cycle of the medium grid (iteration 150 in Fig. 2), the trailing edge ordinates did not change prior to that point. Since the displacement thicknesses were added to the wing ordinates using under-relaxation, the ordinates of the fluid airfoil increased smoothly from the original values once the viscous procedure was initiated. After about 125 iterations on the medium grid (by iteration 225 on the figure), the displacement surface ordinates converged. At iteration 300 the grid was again refined, and the fluid airfoils were not updated again until 50 iterations later. At that point, the magnitude of the trailing edge displacement surface ordinates increased significantly due to the ability of the fine grid to more accurately resolve the sharp increase in displacement thickness, which occurs as the trailing edge is approached. Nevertheless, the results shown in Fig. 2 indicate that the trailing-edge ordinates of the fluid airfoils converged rapidly and were essentially constant at the end of the calculation.

Based upon these results, it is believed that the present viscous transonic wing design method does converge using the procedure outlined. Thus, results obtained with it, at least from a convergence standpoint, should be adequate for engineering calculations.

Verification of the Analysis-Design Method

Viscous Analysis Verification

Theoretical viscous pressure distributions obtained with the present method for a root chord Reynolds number of 15 million for the ONERA M-6 wing are compared to corresponding inviscid results, also obtained with the present code, in Fig. 3. In this case, the freestream Mach number was 0.84 and the angle of attack was 3.06 deg. As can be seen, viscous effects on the lower surface of the ONERA wing were quite small and only noticeable in the vicinity of the trailing edge. On the upper surface, however, inclusion of viscous interaction moved the rear shock wave forward about 5% chord and significantly weakened the shock strength. Also, like the lower surface, the viscous pressures near the trailing edge were less than the inviscid values.

These viscous pressure distributions are compared with experimental data[6] at several span stations in Fig. 4. The experimental data were obtained at the same Mach number and angle of attack as the theoretical results and for an average wing Reynolds number of 11.75 million, which is approximately equivalent to 15 million at the root. On the inboard sections, inclusion of viscous interaction significantly improved the prediction of shock location, shock strength, and trailing-edge pressure variation; but at the outboard stations, the shock positions predicted by the viscous results tended to be slightly upstream from the positions measured experimentally. However, the shock strength predictions were improved

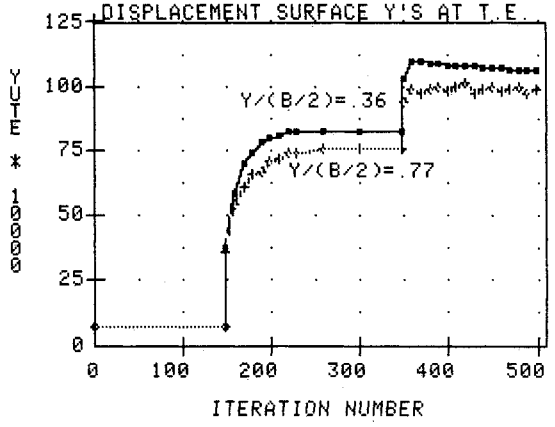

Fig. 2 Variation in trailing edge displacement surface ordinates with iteration number.

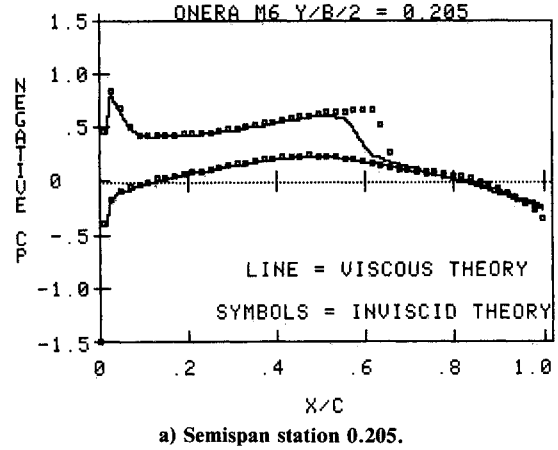

a) Semispan station 0.205.

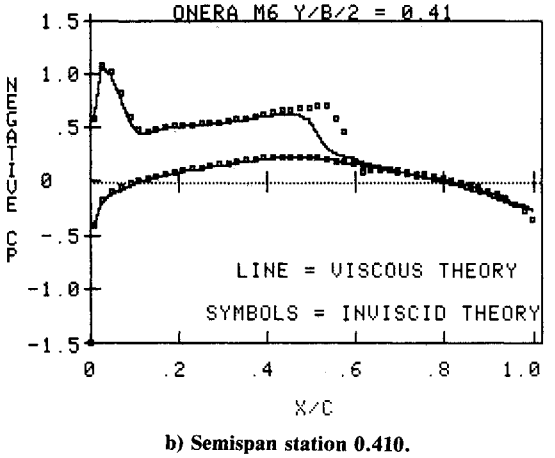

b) Semispan station 0.410.

Fig. 3 Comparison of viscous and inviscid analysis for ONERA M-6 pressure distributions, $M_\infty = 0.84$, $\alpha = 3.06$ deg.

by the inclusion of viscous effects. Interestingly, theoretical viscous results obtained using a root chord Reynolds number of 25 million gave better shock locations at the outboard stations; and it should be noted that similar results have been obtained by other investigators.[5] Unfortunately, the experimental data indicated flow separation near the wing tip, which might affect the outboard station, and accurate values of the experimental lift coefficient and of the tunnel corrections for Mach number and angle of attack were unknown. Nevertheless, the viscous results had the correct trend in that they predicted a lift coefficient lower than the inviscid calculations and in that the shock waves tended to be further forward and weaker.

Typical displacement thickness profiles that correspond to the conditions shown in Fig. 4 are shown in Fig. 5. For these cases, transition was assumed at 6% chord, and the lower surface displacement thicknesses were quite small, which explains the lack of significant viscous effects on the lower surface. On the upper surface, however, the magnitude of the displacement thicknesses was considerably larger, and the presence of the shock wave was indicated by the presence of a bump in the curves. This bump was primarily due to shock boundary layer interaction; its main effect was to move the shock wave forward from the location predicted by an inviscid calculation. As noted previously, the outboard shock locations predicted by the present viscous method were forward of those measured experimentally. While this difference could be due to wing tip and experimental effects not modeled in the present problem, it should also be recognized that the amount of shock boundary layer interaction was controlled by some of the parameters in the program and that these parameters may need further refinement.

Comparison of the total drag with the pressure drag for this case indicated that the viscous drag contribution was essentially constant over the span. Also, the total drag was highest at the inboard sections and decreased steadily towards the wing tip. This trend is in agreement with results obtained by other investigators for this case.[6] Finally, the theoretical wing lift coefficient was 0.238, which is in good agreement with the viscous calculation result of 0.235 reported by Schmitt et al.[5] The corresponding inviscid value obtained with the present method was 0.277. It should be noted that these lift coefficient values and the results shown in Figs. 3 and 5 indicate that, contrary to the assumption of many investigators, viscous effects are significant on low aspect ratio thin wings, such as the ONERA M-6.

As another test of the method, viscous and inviscid analysis results are compared with experimental data[17] for Wing A in Fig. 6. Wing A was a typical "transport" type wing, composed of aft-cambered transonic airfoil sections, and it had the following characteristics: $AR=8$, 1/4 chord sweep = 25 deg, taper = 0.4, and total twist = −4.8 deg. In this case, accurate experimental lift coefficients were known; thus, corrections were made to both the Mach number and angle of attack in order to match the experimental coefficients. In this way, the effect of wind tunnel corrections was approximately included. The best correlation was obtained when the Mach number was decreased from the experimental value of 0.82 to 0.80 and when the angle of attack was reduced from the tunnel angle of 2.5 to 2.0 deg in the viscous case and to 1.2 deg in the inviscid case. Note that the viscous case required a smaller angle-of-attack correction. In addition, as shown in the figure, the inclusion of viscous effects not only improved the predicted magnitude of the shock strengths but also significantly improved the pressure distribution predictions on both the upper and lower surfaces of the aft portions of the wing. However, like the ONERA results, the present viscous calculation predicted shock locations forward of those measured experimentally. Nevertheless, it is believed that these and the ONERA results indicate that the present analysis-design method with viscous interaction can yield improved engineering results for the analysis of the flow about transonic wings.

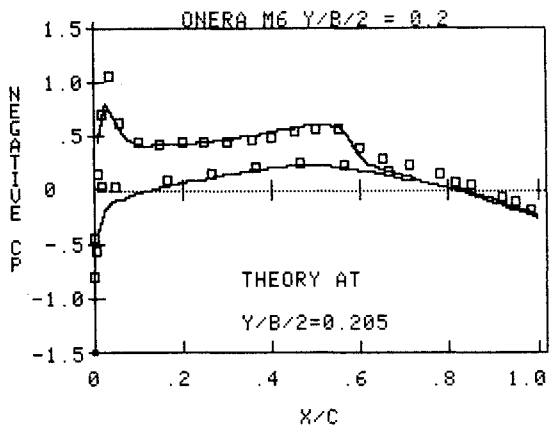

a) Semispan station 0.205.

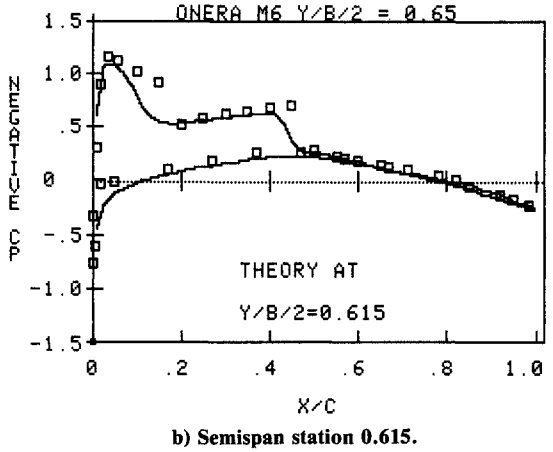

b) Semispan station 0.615.

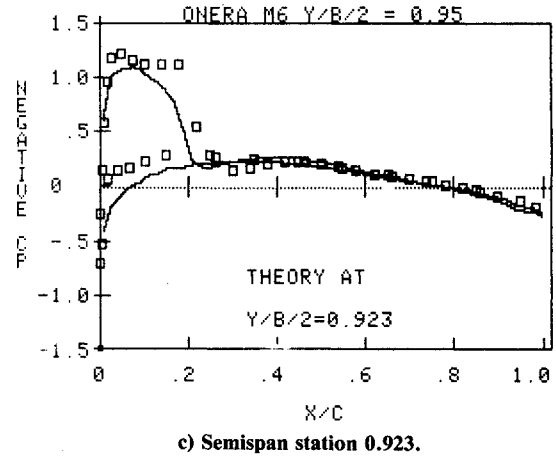

c) Semispan station 0.923.

Fig. 4 Comparison of viscous analysis and experimental data for ONERA M-6 pressure distributions, $M_\infty = 0.84$, $\alpha = 3.06$ deg, RN = 11.75 × 106.

Viscous Design Verification

Since the present viscous analysis-design method could be used to design an entire wing, the upper and lower surfaces of only part of the wing, or the upper or lower surface of part of a wing, many design verification tests could be constructed. However, since the inviscid design portion was thoroughly tested previously[4,18] and the viscous procedure was verified above, only a single design verification test is presented here. In this test, the inverse procedure was used at only one span station and only on the upper surface. This seemingly simple case was selected because it posed the most severe test on the program logic. In this situation, viscous calculations had to be performed on the upper and lower surfaces at all analysis stations and on the lower surface of the design station. The viscous results then had to be coupled to the outer inviscid calculations properly. In addition, automatic relofting was used in this case in order to generate a "closed" airfoil section at the design station.

For this test case, the design station was chosen to be at the 0.615 semispan station of the ONERA M-6 planform. Again, the Mach number was 0.84 and the angle of attack was 3.06 deg, but the root chord Reynolds number was increased to 25 million. The nose shape was determined by the reloft procedure, and an upper surface pressure distribution was specified for the last 80% of the airfoil. Care should be exer-

cised in selecting the shape and the chordwise starting point of the design pressure distribution. Previous studies[8] have indicated that uniqueness problems can occur if the inverse region is started near a supersonic to subsonic shock wave. In addition, the initial 6-10%[9,14] of the leading edge shape must be user-specified and compatible with the desired design pressures at the analysis-design interface. In other words, the design-region pressures near the interface should be similar to those observed for airfoil sections having similar leading edges in order to prevent slope discontinuities at the interface.

The target pressure profile, which is shown in Fig. 7, was arbitrarily chosen as a typical design pressure distribution. It had a supersonic pressure plateau followed by a gentle recompression near 55% chord and a subsequent, almost linear, recovery to the trailing edge. The actual pressures at the design station, which were determined at the end of the computation from the final converged potential flow solution, are also shown in Fig. 7. By comparing this result with that shown in Fig. 4b for the original ONERA M-6 wing, it can be seen that the new pressure profile had a constant plateau after the front oblique shock and that the recovery to subsonic flow was about 10% further aft. As can be seen, the design distribution was essentially indistinguishable from the desired target values.

Figure 8 shows the computed upper surface displacement thickness profile at the design station. Examination of this result revealed that the boundary layer at the trailing edge of the design station was slightly thicker than those at the other stations, primarily as a result of the difference in the pressure recovery near the trailing edge. In addition, the replacement of the shock wave by a more gentle further aft recovery reduced the magnitude of the increase, or bump, in the displacement thickness near the start of the recovery region.

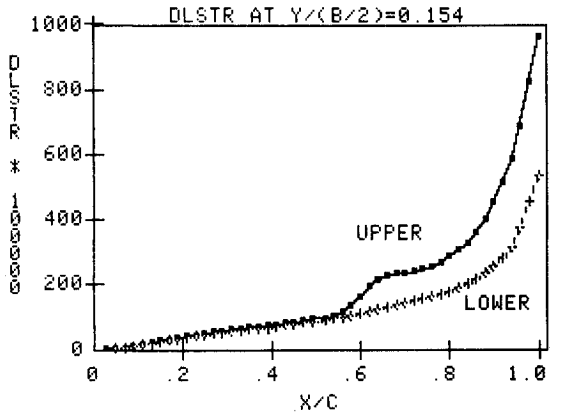

a) Semispan station 0.154.

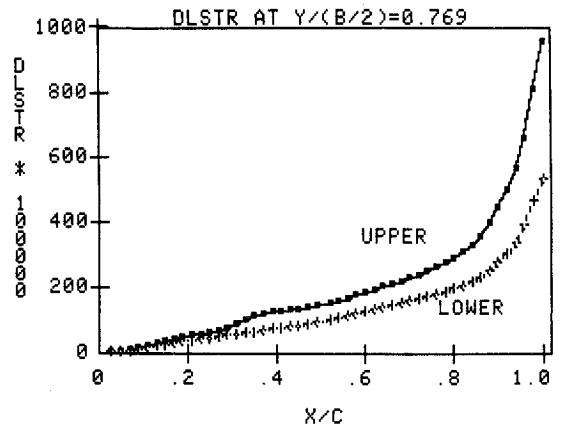

b) Semispan station 0.769.

Fig. 5 Typical displacement thickness profiles at various span stations on the ONERA M-6 wing.

Figure 9 shows on an enlarged vertical scale the fluid airfoil determined by the analysis-design procedure at the design station. On the lower surface, where the original airfoil shape was retained, viscous effects were small, and the fluid or displacement surface corresponded closely to the original airfoil except near the trailing edge. However, on the upper surface, the new pressure distribution yielded via the inverse method an effective displacement surface considerably different than the original section. This new effective section was thicker than the original, 10% vs 9.8%; and the maximum upper surface ordinate was at 49.5% chord rather than at 37.9%.

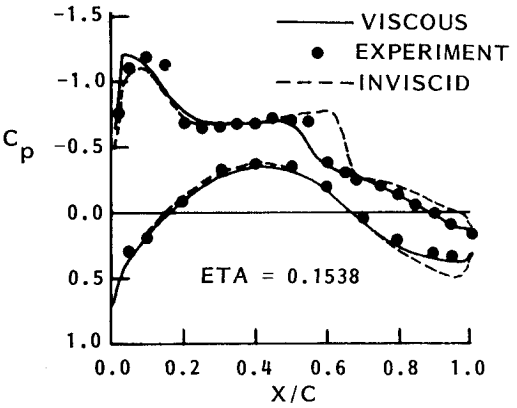

a) Semispan station 0.154.

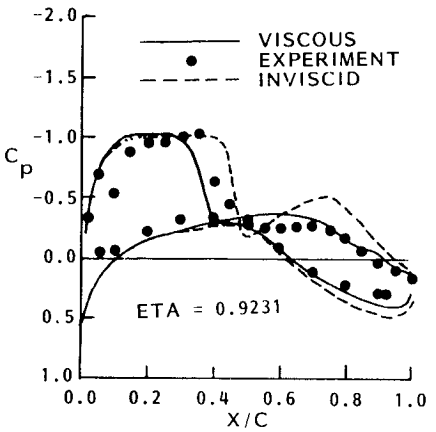

b) Semispan station 0.923.

Fig. 6 Comparison of viscous wing *A* pressure distributions with inviscid analysis and experiment.

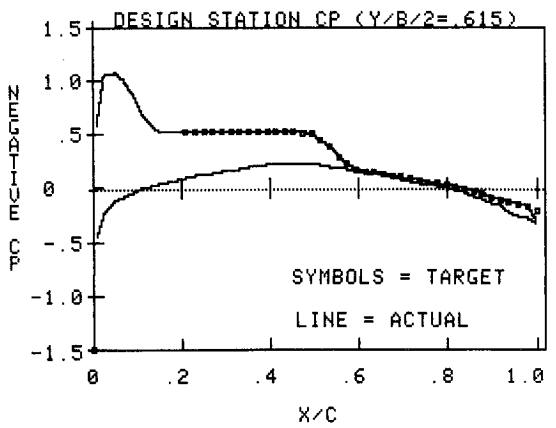

Fig. 7 Comparison of target and actual pressure distributions at the design station.

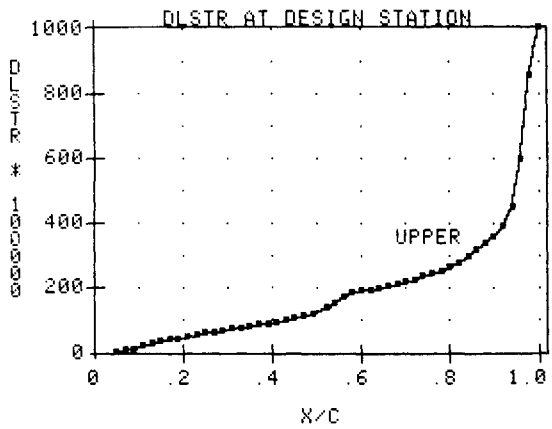

Fig. 8 Upper surface displacement thickness profile at the design station.

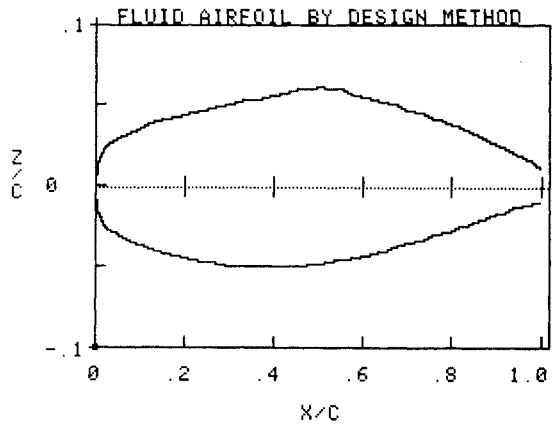

Fig. 9 Enlarged plot of the fluid airfoil determined by the viscous analysis-design method.

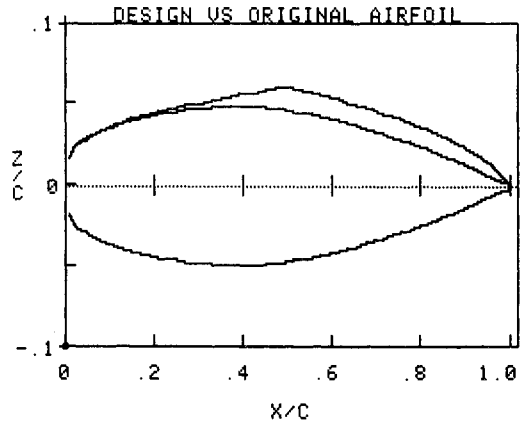

Fig. 10 Comparison of the original ONERA M-6 airfoil section with the section designed by the inverse method.

After the inverse procedure was completed, a boundary layer calculation was automatically performed on the design section. The resultant displacement thicknesses were then appropriately subtracted from the fluid airfoil or displacement surface to determine the actual "hard" airfoil corresponding to the viscous fluid airfoil. Figure 10 compares the original ONERA M-6 airfoil section with the new shape at the design station, again on an enlarged vertical scale. Since the lower surface was not redesigned in this example, it was identical to the original shape. The upper surface, however, was considerably different in that the aft portion was thicker with a maximum thickness of about 10.7% near midchord. In addition, the relofting procedure resulted in a closed trailing edge and, while not obvious, a slightly different upper surface leading edge. The most significant change, however, was in the shape near the midchord point. This unusual profile was the result of the desired pressure recovery between the constant pressure plateau on the forward portion of the wing and the near linear recovery specified on the aft portion of the design section. It is unlikely that this shape could have been conceived without the use of an inverse method with viscous interaction.

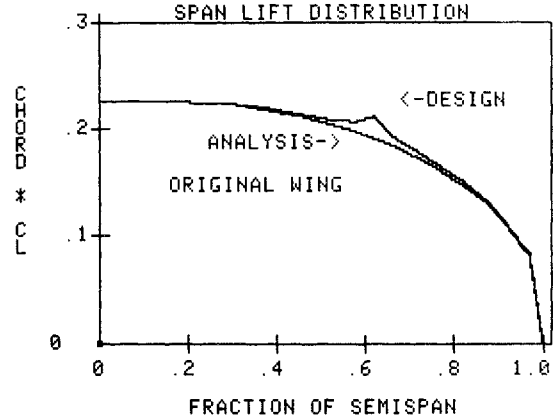

Fig. 11 Comparison of the original ONERA M-6 span lift distribution with that obtained in the design case.

Finally, Fig. 11 compares the span lift distribution for the original ONERA M-6 wing with that obtained from the design test case. As expected, the lift at the design station of 0.615 semispan was increased. In addition, even though a new pressure distribution was prescribed at only one station, the pressures and lift were measurably affected between 0.50 and 0.70 semispan due to three-dimensional and viscous effects.

It is believed that these results verify that the present viscous design method can be used to design airfoil sections on wings in transonic flow which correctly reproduce desired pressure distributions while accounting for the primary effects of viscous interaction.

Conclusion

A direct-inverse transonic wing analysis-design method was developed which includes the effects of weak viscous interaction due to the presence of a turbulent boundary layer on a wing. The resultant method and computer code were verified by comparison with experimental data. It was shown that viscous effects are significant on thin low-aspect ratio wings as well as on transport-type wings and that by including viscous effects improved analysis and design results can be obtained. This new method should be adequate for transonic aerodynamic studies associated with preliminary analysis and design.

Acknowledgments

The work presented in this paper was part of a joint effort by the Lockheed-Georgia Company and Texas A&M University for the Naval Air Systems Command Under Navy Contract N0167-81-C0078-P00004. The overall project was under the direction of D. G. Kirkpatrick (NAVAIR 311D), and the overall contract monitor was Dr. T. C. Tai of the David Taylor Naval Ship Research and Development Center. The Texas A&M University portion of the project was under Contract CA088757 between the Lockheed-Georgia Company and the Texas A&M Research Foundation. The resultant computer program is available to qualified requestors.

References

[1]Lores, M. E. and Hinson, B. L., "Transonic Design Using Computational Aerodynamics," *Progress in Aeronautics and*

Astronautics: Transonic Aerodynamics, edited by D. Nixon, Vol. 22, AIAA, NY, 1982, pp. 377-398.

[2]Henne, P.A., "Inverse Transonic Wing Design Method," *Journal of Aircraft,* Vol. 18, Feb. 1981, pp. 121-127.

[3]Shankar, V., Malmuth, N. D., and Cole, J. D., "Computational Transonic Design Procedure for Three-Dimensional Wings and Wing Body Combinations," AIAA Paper 79-0322, Jan. 1979.

[4]Weed, R.A., Carlson, L.A., and Anderson, W.K., "A Combined Direct Inverse Three-Dimensional Transonic Wing Design Method for Vector Computers," AIAA Paper 84-2156, Aug. 1984.

[5]Schmitt, V., Destarac, D., and Chaumet, B., "Viscous Effects on a Swept Wing in Transonic Flow," AIAA Paper 83-1804, July 1983.

[6]Schmitt, V., and Charpin, D., "Pressure Distributions on the ONERA M-6 Wing at Transonic Mach Numbers," *Experimental Data Base for Computer Program Assessment,* Appendix B1, North Atlantic Treaty Organization Advisory Group for Aerospace Research and Development, Paris, France, AGARD-AR-138, May 1979, pp. B1-1-B1-44.

[7]South, J. C., Keller, J. D., and Hafez, M., "Vector Processor Algorithms for Transonic Flow Calculations," *AIAA Journal,* Vol. 18, July 1980, pp. 786-792.

[8]Purcell, T. W. and Carlson, L. A., "Transonic Airfoil Design and Analysis Using the Full Potential Equation and Approximate Boundary Conditions," Texas A&M Research Foundation, College Station, TX, Rept. TAMRF-4276-8101, Aug. 1981.

[9]Anderson, W. K. and Carlson, L. A., "Inverse Wing Design on a Vector Computer," Texas A&M Research Foundation, College Station, TX, Rept. TAMRF-4534-8218, Dec. 1982.

[10]Weed, R. A., Carlson, L. A., and Anderson, W. K., "Combined Direct Inverse Three-Dimensional Transonic Wing Design," David Taylor Naval Ship Research and Development Center, Bethesda, MD, DTNSRDC-ASED-CR-03-83, May 1983.

[11]Newman, P. A., Carter, J. E., and Davis, R. M., "Interaction of a Two-Dimensional Strip Boundary Layer with a Three-Dimensional Transonic Swept Wing Code," NASA TM-78640, 1978.

[12]Nash, J. F. and Tseng, R. R., "The Three-Dimensional Turbulent Boundary Layer on an Infinite Yawed Wing," *The Aeronautical Quarterly,* Nov. 1971, pp. 346-362.

[13]Nash, J. F., and Macdonald, A. G. J., "The Calculation of Momentum Thickness in a Turbulent Boundary Layer at Mach Numbers Up to Unity," Aeronautical Research Council C.P. 963, London, England, 1967.

[14]Carlson, L. A., "TRANDES: A Fortran Program for Transonic Airfoil Analysis or Design," NASA CR-2821, June 1977.

[15]Carlson, L. A., "TRANSEP: A Program for High Lift Separated Flow About Airfoils," NASA CR-3376, Dec. 1980.

[16]Whitfield, D. L., and Janus, J. M., "Three-Dimensional Unsteady Euler Equation Solution Using Flux Vector Splitting," AIAA Paper 84-1552, June 1984.

[17]Hinson, B. L., and Burdges, K. P., "Acquisition and Application of Transonic Wing and Far-Field Test Data for Three-Dimensional Computational Method Evaluation," AFOSR-TR-80-0421, March 1980.

[18]Weed, R. A., and Carlson, L. A., "Combined Direct/Inverse Three-Dimensional Wing Design with Viscous and Wing Body Effects," David Taylor Naval Ship Research and Development Center, Bethesda, MD, DTNSRDC-ASED-CR-02-84, Feb. 1986.